Nucleotide-binding oligomerization domain (NOD) signaling defects and cell death susceptibility cannot be uncoupled in X-linked inhibitor of apoptosis (XIAP)-driven inflammatory disease

Received for publication, February 14, 2017, and in revised form, April 3, 2017 Published, Papers in Press, April 12, 2017, DOI 10.1074/jbc.M117.781500

Steven M. Chirieleison[‡1], Rebecca A. Marsh[§], Prathna Kumar[‡], Joseph K. Rathkey[‡], George R. Dubyak[¶], and Derek W. Abbott[‡2]

From the Departments of [‡]Pathology and [¶]Physiology and Biophysics, Case Western Reserve University School of Medicine, Cleveland, Ohio 44106 and the [§]Division of Bone Marrow Transplantation and Immune Deficiency, Cincinnati Children's Hospital, Cincinnati, Ohio 45229

Edited by Luke O'Neill

The X-linked inhibitor of apoptosis (XIAP) protein has been identified as a key genetic driver of two distinct inflammatory disorders, X-linked lymphoproliferative syndrome 2 (XLP-2) and very-early-onset inflammatory bowel disease (VEO-IBD). Molecularly, the role of XIAP mutations in the pathogenesis of these disorders is unclear. Recent work has consistently shown XIAP to be critical for signaling downstream of the Crohn's disease susceptibility protein nucleotide-binding oligomerization domain-containing 2 (NOD2); however, the reported effects of XLP-2 and VEO-IBD XIAP mutations on cell death have been inconsistent. In this manuscript, we describe a CRISPR-mediated genetic system for cells of the myeloid lineage in which XIAP alleles can be replaced with disease-associated XIAP variants expressed at endogenous levels to simultaneously study inflammation-related cell death and NOD2 signaling. We show that, consistent with previous studies, NOD2 signaling is critically dependent on the BIR2 domain of XIAP. We further used this system to reconcile the aforementioned inconsistent XIAP cell death data to show that XLP-2 and VEO-IBD XIAP mutations that exhibit a loss-of-function NOD2 phenotype also lower the threshold for inflammatory cell death. Last, we identified and studied three novel patient XIAP mutations and used this system to characterize NOD2 and cell death phenotypes driven by XIAP. The results of this work support the role of XIAP in mediating NOD2 signaling while reconciling the role of XLP-2 and VEO-IBD XIAP mutations in inflammatory cell death and provide a set of tools and framework to rapidly test newly discovered XIAP variants.

The avoidance of inflammatory disease requires exquisite control of innate immune and inflammatory signaling. The NOD2:RIPK2 innate immune signaling axis provides an example of this tight control, as loss-of-function (LOF)[3] NOD2 alleles are linked to genetic Crohn's disease, whereas gain-of-function NOD2 alleles cause early-onset sarcoidosis (1–7). Importantly, even in patients not harboring mutations in NOD2, NOD2 and its obligate protein kinase-binding partner, RIPK2, are NF-κB-controlled genes. NOD2 and RIPK2 are therefore often up-regulated in inflammatory disease and are thought to contribute to the pathogenesis of a number of inflammatory disorders (6, 8–13). Thus, there is a fine balance of NOD2 and RIPK2 signaling that must be achieved to coordinate a balanced immune response. Too much signaling causes inflammatory disease, and too little signaling also causes inflammatory disease. Given the role of posttranslational modifications, especially ubiquitination, in regulating NOD2 signaling activity (reviewed in Ref. 14), it becomes imperative to understand how ubiquitination pathways maintain proper signaling and proper immunologic homeostasis.

A key E3 ubiquitin ligase implicated in NOD:RIPK2 signaling is the X-linked inhibitor of apoptosis protein (XIAP) (15, 16). Mutations in XIAP cause both X-linked lymphoproliferative disorder (XLP-2) and very-early-onset inflammatory bowel disease (VEO-IBD) (17, 18). Functionally, XIAP relies on RING-mediated ubiquitin transfer to regulate a diverse set of cellular processes (reviewed in Ref. 19). Originally described as an inhibitor of cell death proteases (20), XIAP has been demonstrated to be a critical regulator of caspase activation and activity (21–25). Extensive work has further demonstrated XIAP to play a pivotal role in a number of other cellular processes, including copper homeostasis (26–28), autophagy (29, 30), and

This work was supported by National Institutes of Health Grants R01 GM086550 and P01 DK091222 (to D. W. A.). The authors declare that they have no conflicts of interest with the contents of this article. The content is solely the responsibility of the authors and does not necessarily represent the official views of the National Institutes of Health.

This article contains supplemental Figs. 1 and 2.

[1] Supported by Case Western Reserve University National Institutes of Health Medical Scientist Training Program Grant T32 GM007250 and Case Western Reserve University Immunology Training Program Grant T32 AI089474.

[2] To whom correspondence should be addressed: Rm. 6531, Wolstein Research Bldg., 2103 Cornell Rd., Cleveland, OH 44106. Tel.: 216-368-8564; E-mail: dwa4@case.edu.

[3] The abbreviations used are: LOF, loss-of-function; XIAP, X-linked inhibitor of apoptosis; XLP-2, X-linked lymphoproliferative syndrome 2; VEO-IBD, very-early-onset inflammatory bowel disease; PBMC, peripheral blood mononuclear cell; BMDM, bone marrow-derived macrophage; NOD, nucleotide oligomerization domain; iBMDM, immortalized bone marrow-derived macrophage; Neg, non-targeted CRISPR cell line; L18-MDP, L18 muramyl dipeptide; nec-1, necrostatin-1; PI, propidium iodide; PAM, protospacer-adjacent motif, Z-VAD, benzyloxycarbonyl-VAD; MLKL, mixed lineage kinase domain-like; sgRNA, single-guide RNA.

restriction of bacterial proliferation *in vitro* and *in vivo* (31–33). Structurally, XIAP contains three baculoviral inhibitor of apoptosis repeat domains (BIR1, BIR2, and BIR3), an ubiquitin-binding domain, and a C-terminal RING domain that confers E3 ubiquitin ligase activity (34–38). XIAP mutations linked to XLP-2 and VEO-IBD are dispersed throughout the gene and cause either truncation of the protein or amino acid substitutions. Numerous independent groups have shown that truncation mutants that delete the RING domain and point mutants that disrupt the BIR2 domain greatly decrease NOD:RIPK2 signaling. These results have been consistent between studies and have utilized primary patient peripheral blood mononuclear cells (PBMCs) as well as a well known XIAP-null colon carcinoma cell line ($XIAP^{-/Y}$ HCT-116) (18, 39–41).

Less consistent have been the results studying the roles of XLP-2 and VEO-IBD XIAP mutations in inflammation-related cell death. Studies with primary bone marrow-derived macrophages (BMDMs) from mice genetically null for XIAP have clearly shown them to be hypersensitive to cell death following stimulation with a variety of inflammatory ligands such as TNF and LPS (42, 43); however, because it relies on primary cell generation, the system is not easily amenable to genetic manipulation. For this reason, reconstitution experiments with XLP-2 or VEO-IBD mutations have not been performed. Cell death in XLP-2 and VEO-IBD patient primary cells and in XLP-2 and VEO-IBD patient tissue has been studied, but these studies have been limited to CD3+ T cells and intestinal epithelial cells and have been inconsistent. For instance, in one study, increased intestinal lamina propria T cell apoptosis was seen; however, of the 10 patient biopsies studied, 4 had overlapping cell death frequencies with unaffected control tissue (39). Another study reported no increased T cell apoptosis (40) whereas yet another showed increased T cell apoptosis in a single patient (18). In only one of these studies was a particular patient mutation correlated with apoptosis, and it is therefore difficult to determine from the literature which XIAP mutations cause apoptosis susceptibility. XIAP mutant intestinal epithelial cell apoptosis studies have likewise been inconsistent. One study using immunohistochemical techniques showed no increased apoptosis, whereas a reconstitution study in an immortalized XIAP-deficient colon carcinoma cell line ($XIAP^{-/Y}$ HCT-116) showed that XIAP mutations actually confer a degree of protection against TNF-related apoptosis-inducing ligand (TRAIL)-induced apoptosis compared with genetic loss of XIAP (39, 41). The discordance in susceptibility to cell death between patient samples and across cell types is potentially the result of genetic heterogeneity among patients, differing treatment regimens among patients, differing patient disease courses, and different techniques and agonists used in each study. Although these human studies are incredibly important to understand human pathophysiology, caveats present in all human studies make identification of molecular mechanisms more difficult.

XIAP-null BMDMs have a very strong cell death phenotype (42, 43), and coupled with the facts that NOD2 signaling is strongest in the macrophage/dendritic cell lineage (44–46) and that hematopoietic stem cell transplant has been curative in XIAP-driven XLP-2 and VEO-IBD (18, 47–49), systematic study of XIAP mutants in the myeloid lineage is important for the field but has yet to be performed. In this work, we generate XIAP knockout macrophages and dendritic cells. We show that these cells recapitulate the published NOD2 signaling defect and allow systematic study of the role of XIAP in inflammatory cell death in the myeloid lineage. We show that XIAP-null macrophages preferentially undergo apoptosis in response to inflammatory stimuli, whereas XIAP-null dendritic cells undergo both apoptosis and necroptosis. We reconstitute these cells with the three major XIAP truncation mutants as well as point mutations from each of the BIR domains at near endogenous levels. We employ these reconstituted cells to show that mutants that cause NOD2 signaling loss also cause inflammatory cell death susceptibility, whereas those that do not affect NOD2 signaling also do not affect inflammatory cell death susceptibility. Last, we identify and utilize three novel XLP-2-linked XIAP mutations to predict and study mutant function. In all, this work supports the published role of XIAP in NOD2:RIPK2 signaling. This system allows the rapid interrogation of newly discovered XIAP variants for functional deficits. Further, these findings resolve important inconsistencies concerning the role XIAP mutations play in inflammatory cell death susceptibility and provide a platform to study the molecular biology of novel XIAP mutants.

Results

Genetic XIAP loss causes a blunted NOD1/2 response

The investigation of XIAP loss in innate immune signaling pathways has been somewhat limited by the reagents available. Two immortalized cell lines in which XIAP is genetically lost, $XIAP^{-/-}$ MEFs and $XIAP^{-/Y}$ HCT116 cells, have less-than-robust responses to toll-like receptor (TLR) and NOD stimuli compared with macrophages and dendritic cells. Mutant reconstitution in primary cells from $XIAP^{-/-}$ mice and subsequent study of those cells is difficult because of the limited proliferative capacity of primary cells, and the study of XIAP-mutated patient cells is limited by both the availability of primary patient cells and the limited amount of blood that can be drawn from these young patients. Given these difficulties and the need to reconcile variable reports of inflammatory cell death phenotypes in XIAP-mutant cells, we coupled CRISPR/Cas9 with our recently published myeloid lentiviral expression system (50) to generate a cell culture system in which the function of XIAP could be directly assessed. Stable knockout cell lines were generated using the LentiCrisprV2 system (51) with efficient loss of XIAP in HEK293Ts, a murine dendritic cell line (DC2.4s), and immortalized bone marrow-derived macrophages (iBMDMs) with two distinct single-guide RNA (sgRNA)-targeting constructs (G1 and G2) (Fig. 1*a*). Utilizing the HEK293T XIAP knockout cells lines, we then tested whether loss of XIAP impaired NOD1- and NOD2-driven transcriptional responses. NOD1 or NOD2 overexpressed in HEK293Ts lacking XIAP in the presence of an NF-κB-driven luciferase demonstrated blunted NF-κB-driven luciferase activity consistent with the known function of XIAP at NOD1 and NOD2 signaling complexes (15, 16) (Fig. 1*b*). To confirm that this defect was consistent with a loss of endogenous NOD2-driven transcription activity, dendritic cells with (Neg) or without (XIAP-G1 and XIAP-G2) XIAP were stimulated

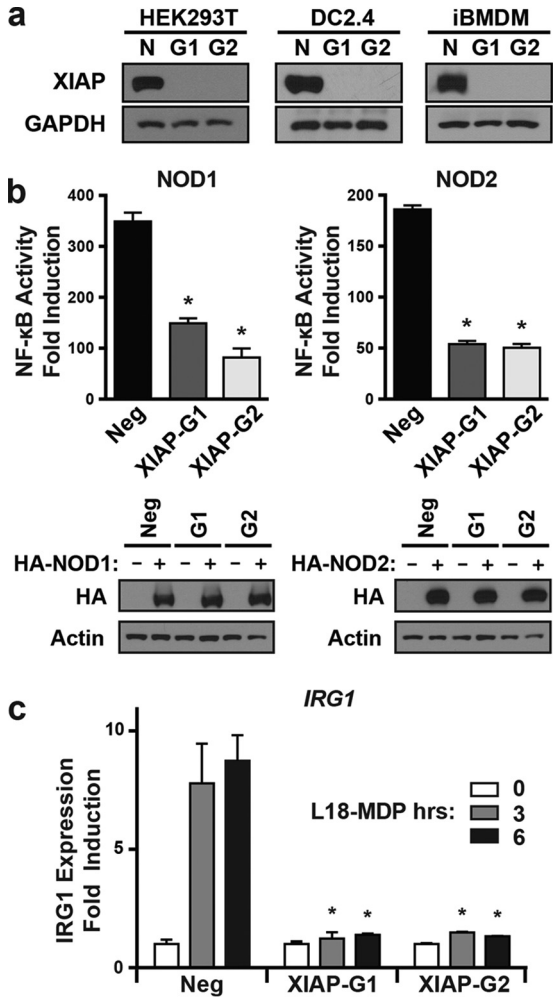

Figure 1. CRISPR/Cas9 knockout of XIAP blunts NOD1/2 response. *a*, Western blots showing CRISPR/Cas9-mediated XIAP knockout in the HEK293T, DC2.4, and iBMDM cell lines. *N*, non-targeted: *G1, XIAP-G1; G2, XIAP-G2*. *b*, *top panels*, NOD1 and NOD2-activated NF-κB luciferase assay in non-targeted (*Neg*) or stable XIAP knockout HEK293T lines (*XIAP-G1* and *XIAP-G2*). *Bottom panels*, Western blots from a single replicate of the luciferase assay above, demonstrating equal transfection efficiency for HA-NOD1 and HA-NOD2 in the cell lines examined for NOD-induced NF-κB activity. *, $p \leq 0.05$ compared with Neg by two-way ANOVA. *c*, real-time quantitative PCR for expression of IRG1 in Neg or XIAP knockout DC2.4 cells treated with 10 μg/ml of L18-MDP for 0, 3, and 6 h. *, $p \leq 0.05$ compared with the corresponding Neg time point by two-way ANOVA.

with the NOD2 agonist L18-muramyl dipeptide (L18-MDP) and assayed for the expression of IRG1, a downstream transcription target we have demonstrated previously as a NOD2-responsive gene (52). As seen in the NF-κB luciferase assays, loss of XIAP blunted the NOD2-driven expression of immune-regulated genes, evidenced by significantly lower MDP-induced expression of IRG1 in dendritic cells lacking XIAP (Fig. 1*c*). Taken together, these cell lines recapitulate signaling defects at innate receptors known to require XIAP activity and provide a platform to dissect XIAP function.

XIAP is a critical regulator of cell death in dendritic cells and macrophages

XIAP functions as a diverse mediator of many different cellular processes (reviewed in Ref. 19), including the direct inhibition of caspases 3, 7, and 9 to restrict cell death (42, 25, 53). Reports on cell death in XIAP-mutant patients have been inconsistent. Some studies have found increased cell death. Others have found no change in cell death, whereas still others have shown some degree of protection from cell death from XIAP-mutant alleles. Given that the studies on the XIAP mutants had been performed in T cells and in intestinal epithelial cells, and given that the myeloid lineage is known to be extremely sensitive to cell death when XIAP is lost, we tested our XIAP$^{-/-}$ macrophages and dendritic cells for a cell death phenotype. To elicit cell death, cells were treated with TNF and the IAP antagonist GDC-0152. GDC-0152 is a multivalent IAP antagonist with greater collective affinity for cIAP1 and cIAP2 than XIAP, leading to rapid degradation of cIAP1/2 and release of caspase-8 inhibition at the TNF receptor complex (54–56). Loss of XIAP (XIAP-G1 and XIAP-G2) in the DC2.4 cell line resulted in a loss of viable cells following TNF and GDC-0152 treatment relative to the non-targeted (Neg) DC2.4 cell line (Fig. 2*a*). Western blots of cell lysates from Neg, XIAP-G1, and XIAP-G2 DC2.4 cells treated with TNF and GDC-0152 for 0, 8, 16, and 24 h revealed that, although DC2.4 cells undergo a significant level of apoptosis (as indicated by caspase-3 cleavage), necroptosis is also active, as evidenced by elevated and induced phosphorylation of mixed lineage kinase domain-like (MLKL) (57) (Fig. 2*b*). In addition to TNF-stimulated cell death, treatment of DC2.4s with LPS and GDC-0152 resulted in a significant decrease in viable cells with the loss of XIAP (Fig. 2*c*). As seen with TNF treatment, LPS and GDC-0152 treatment resulted in accelerated accumulation of cleaved caspase-3 and slightly elevated phosphorylated MLKL, again indicating that loss of XIAP in dendritic cells increases sensitivity to pro-apoptotic and pro-necroptotic cell death signals (Fig. 2*d*). To examine whether loss of XIAP increased sensitivity to cell death signals in other cell types, iBMDM cells, an immortalized mouse macrophage cell line, were similarly treated with either TNF (Fig. 2*e*) or LPS (Fig. 2*g*) with and without GDC-0152. As was seen with DC2.4s, iBMDMs lacking XIAP exhibited accelerated loss of viable cells. In contrast to the DC2.4s, the TNF- or LPS-stimulated iBMDM cell death was exclusively due to apoptosis rather than necroptosis, as evidenced by increased cleaved caspase-3 but absent phosphorylated MLKL at each time point (Fig. 2, *f* and *h*). Collectively, these results demonstrate that XIAP is a critical regulator of both NOD2 signaling activity as well as TNF- and LPS-driven cell death in both dendritic cells and macrophages.

XIAP sets a critical threshold for apoptosis and necroptosis

To further assess the mechanism by which the DC2.4 and iBMDM XIAP knockout cell lines undergo cell death, a chemical inhibitor approach was utilized. By combining different inhibitors with TNF and IAP antagonist stimulation, cells can be directed toward unique cell death programs. Addition of the pan-caspase inhibitor Z-VAD blocks caspase-8-mediated activation of apoptosis, shunting cells toward RIP1/RIP3-driven necroptosis (58). Alternatively, addition of the RIPK1 inhibitor necrostatin-1 (nec-1) (59) inhibits RIPK1-driven cell death programs, including necroptosis. With this approach, it is possible to decipher whether cells undergo apoptosis, necroptosis, or a combination of both upon TNF-driven cell death initiation.

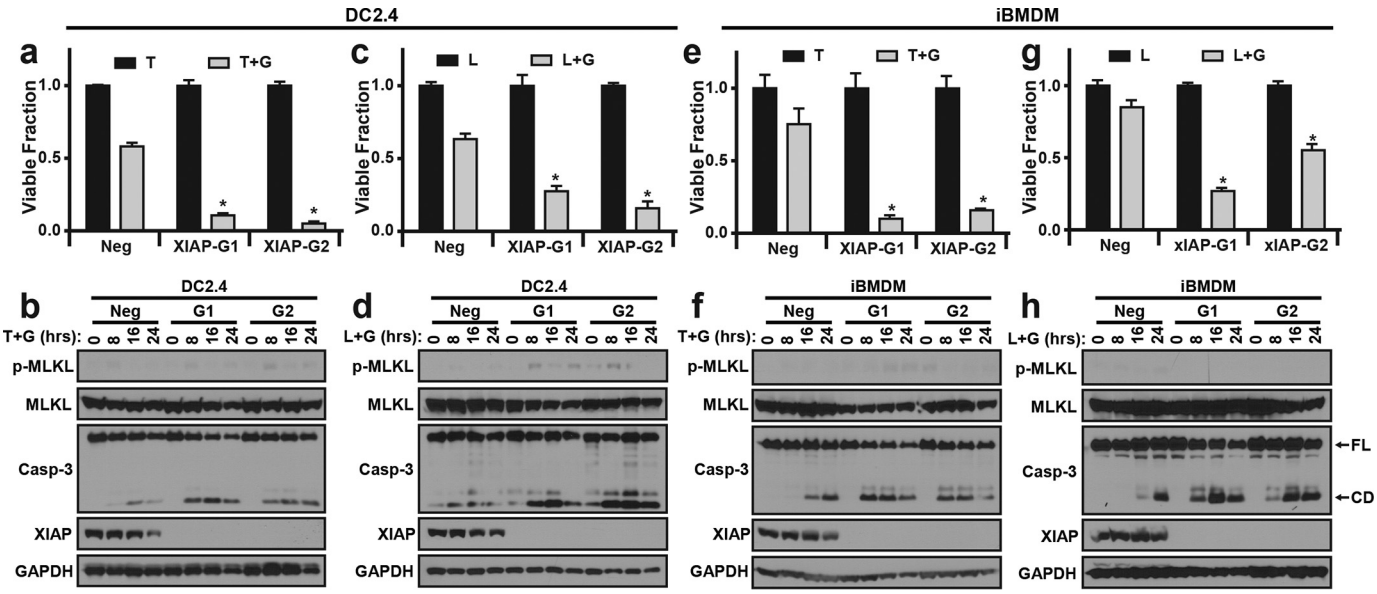

Figure 2. Loss of XIAP sensitizes dendritic cells and bone marrow-derived macrophages to TNF and LPS-induced cytotoxicity. a, non-targeted (*Neg*) and XIAP knockout (*XIAP-G1* and *XIAP-G2*) DC2.4 cell lines stimulated with TNF in the presence (*T*+*G*) or absence (*T*) of the IAP antagonist GDC-0152 for 20–24 h and subsequently stained and quantified for viable cells with methylene blue. *, $p \leq 0.05$ compared with the corresponding Neg by two-way ANOVA. *b*, Western blots of lysates from DC2.4 Neg, XIAP-G1, and XIAP-G2 cell lines stimulated for 0, 8, 16, and 24 h with TNF and GDC-0152. *c*, Neg and XIAP knockout DC2.4 cell lines stimulated with LPS in the presence (*L*+*G*) or absence (*L*) of the IAP antagonist GDC-0152 for 20–24 h. Viable cells were quantified by methylene blue staining *, $p \leq 0.05$ compared with the corresponding Neg by two-way ANOVA. *d*, Western blots of lysates from the DC2.4 Neg, XIAP-G1, and XIAP-G2 cell lines stimulated for 0, 8, 16, and 24 h with LPS and GDC-0152. *e*, Neg, XIAP-G1, and XIAP-G2 stable iBMDM cell lines were stimulated with TNF in the presence (*T*+*G*) or absence (*T*) of the IAP antagonist GDC-0152 for 20–24 h and stained with methylene blue, and viable cells were quantified. *, $p \leq 0.05$ compared with the corresponding Neg treatment by two-way ANOVA. *f*, Western blots of lysates from Neg, XIAP-G1, and XIAP-G2 stable iBMDM cells stimulated with TNF and GDC-0152 for 0, 8, 16, and 24 h. *g*, Neg, XIAP-G1, and XIAP-G2 stable iBMDM cell lines stimulated with LPS in the presence (*L*+*G*) or absence (*L*) of the IAP antagonist GDC-0152 for 20–24 h and methylene blue-stained. *, $p \leq 0.05$ compared with the corresponding Neg treatment by two-way ANOVA. *h*, Western blots of lysates from iBMDM cell lines following stimulation with LPS and GDC-0152 for the indicated time. All Western blot experiments were performed in triplicate. *a*—*d*, TNF (10 ng/ml), GDC-0152 (2 μM), and LPS (100 ng/ml). *e*—*h*, TNF (10 ng/ml), GDC-0152 (200 nM), and LPS (100 ng/ml). *FL*, full-length caspase-3; *CD*, cleaved caspase-3.

Stimulation of DC2.4 dendritic cells with TNF and GDC-0152 in the presence of the pan-caspase inhibitor Z-VAD resulted in sustained cell death that was rescued with the RIPK1 inhibitor nec-1 (Fig. 3*a*). Western blots of lysates from DC2.4 cells treated with TNF and GDC-0152 and either Z-VAD, nec-1, or Z-VAD and nec-1 showed that the prominent apoptotic mechanism of death was entirely diverted to necroptosis, and both pathways were prominently inhibited with the addition of both Z-VAD and nec-1 (Fig. 3*b*). This pattern of cell death was conserved when DC2.4 cells were treated with LPS in place of TNF (Fig. 3, *c* and *d*), indicating that TNF- and LPS-induced cell death in dendritic cells is primarily apoptosis-driven while continuing to be necroptosis-permissive. In contrast to the dendritic cells, iBMDM cell death driven by both TNF and LPS was rescued by both Z-VAD and nec-1 (Fig. 3, *e* and *g*, respectively). This was further substantiated by Western blots of iBMDM cells treated with TNF and LPS in the presence or absence of Z-VAD and nec-1, showing a dramatic reduction of cleaved caspase-3 in the XIAP knockout lines in the presence of the inhibitors (Fig. 3, *f* and *h*).

Throughout the cell death studies, increased phosphorylated MLKL could be visualized in the XIAP-null DC2.4 dendritic cell lines (Figs. 2, *b* and *d*, and 3, *b* and *d*). As necroptosis plays a prominent role in pediatric intestinal inflammation (60), we decided to further examine the effect of XIAP loss on necroptotic cell death. We hypothesized that XIAP may control the threshold for onset of necroptosis by restricting the kinetics of MLKL phosphorylation and subsequent membrane disruption. To test this, we examined the phosphorylation of MLKL in response to TNF, GDC-0152, and Z-VAD treatment in the absence or presence of nec-1 at early time points of treatment. Loss of XIAP (G1 and G2) consistently resulted in increased phosphorylated MLKL at 2 h of treatment and sustained phosphorylated MLKL at 4 h of treatment compared with non-targeted (Neg) cells (Fig. 4*a*). To test whether the early and increased phosphorylated MLKL seen in the XIAP knockout lines was functionally consequential, we performed propidium iodide (PI) uptake assays. Cells were cultured in imaging medium in the presence of PI on a plate reader. After a brief period to read the background PI signal, either TNF alone or TNF, GDC-0152, and Z-VAD was added to the cells, and the PI signal was recorded at 10-min intervals. TNF, GDC-0152, and Z-VAD treatment resulted in an increased PI signal starting ~2 h after addition of treatment, corresponding with phosphorylation of MLKL and disruption of the outer plasma membrane. Importantly, loss of XIAP resulted in a significantly greater PI signal compared with non-targeted cells (Fig. 4*b*). These data demonstrate that XIAP is a critical regulator of TNF- and LPS-induced cell death in dendritic cells and macrophages. Genetic loss of XIAP results not only in a dramatically blunted NOD1/2 response, but it also sensitizes cells to pro-apoptotic and pro-necroptotic stimuli. Given that cells lacking XIAP exhibit this dual phenotype, both or either cellular phenotype may play a critical role in inflammatory disease in which XIAP is mutated.

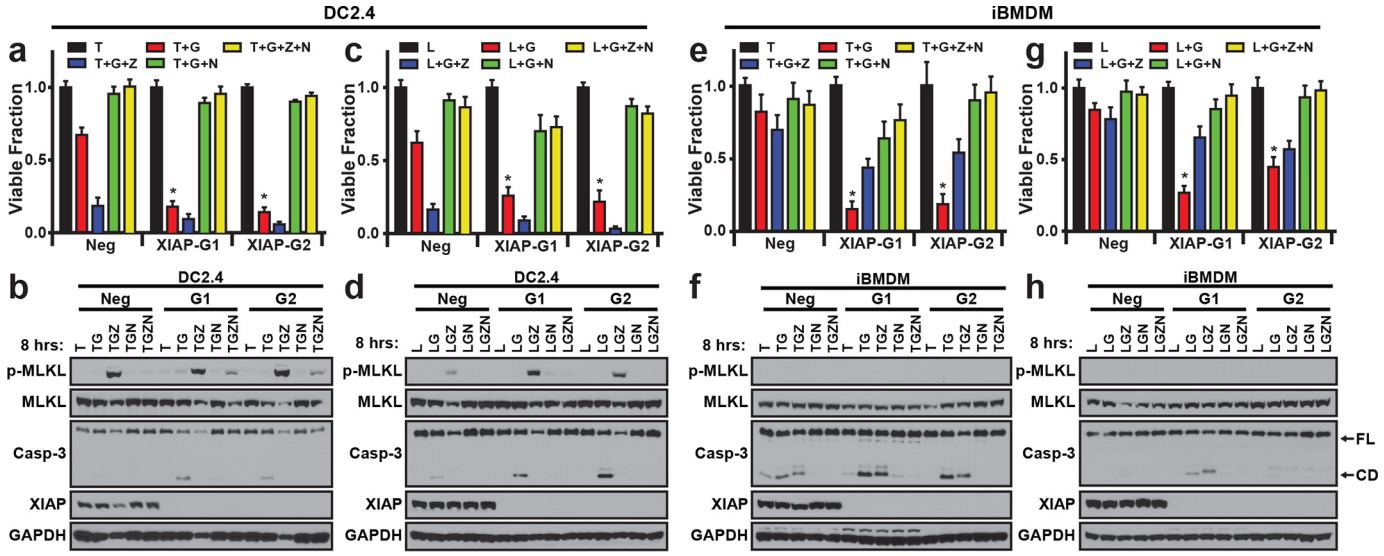

Figure 3. Chemical inhibitor studies reveal that dendritic cells undergo apoptosis and necroptosis, whereas macrophages primarily undergo apoptosis. *a*, non-targeted (*Neg*) and XIAP knock-out (*XIAP-G1* and *XIAP-G2*) DC2.4 cell lines stimulated with TNF (*T*); TNF and GDC-0152 (*T*+*G*); TNF, GDC-0152, and Z-VAD (*T*+*G*+*Z*); TNF, GDC-0152, and nec-1 (*T*+*G*+*N*); or TNF, GDC-0152, Z-VAD, and nec-1 (*T*+*G*+*Z*+*N*) for 20–24 h were methylene blue-stained and quantified. *, $p \leq 0.05$ compared with the corresponding Neg treatment. *b*, Western blots of Neg, XIAP-G1, and XIAP-G2 DC2.4 stable lines following stimulation with either TNF (*T*); TNF and GDC-0152 (*TG*); TNF, GDC-0152, and Z-VAD (*TGZ*); TNF, GDC-0152, and nec-1 (*TGN*); or TNF, GDC-0152, Z-VAD, and nec-1 (*TGZN*) for 8 h. *c*, quantification of Neg, XIAP-G1, and XIAP-G2 DC2.4 stable cell lines stimulated with either LPS (*L*); LPS and GDC-0152 (*L*+*G*); LPS, GDC-0152, and Z-VAD (*L*+*G*+*Z*); LPS, GDC-0152, and nec-1 (*L*+*G*+*N*); or LPS, GDC-0152, Z-VAD, and nec-1 (*L*+*G*+*Z*+*N*) and methylene blue-stained. *, $p \leq 0.05$ compared with the corresponding Neg treatment. *d*, Western blots of Neg, XIAP-G1, and XIAP-G2 DC2.4 cell response to 8-h treatment with either LPS (*L*); LPS and GDC-0152 (*LG*); LPS, GDC-0152, and Z-VAD (*LGZ*); LPS, GDC-0152, and nec-1 (*LGN*); or LPS, GDC-0152, Z-VAD, and nec-1 (*LGZN*). *e*, Neg, XIAP-G1, and XIAP-G2 stable iBMDM cell lines stimulated with either TNF; TNF and GDC-0152; TNF, GDC-0152, and Z-VAD; TNF, GDC-0152, and nec-1; or TNF, GDC-0152, Z-VAD, and nec-1 for 20–24 h were methylene blue-stained and quantified. *, $p \leq 0.05$ compared with the corresponding Neg treatment. *f*, Western blots analyzing Neg, XIAP-G1, and XIAP-G2 stable iBMDM cell lines treated with TNF; TNF and GDC-0152; TNF, GDC-0152, and Z-VAD; TNF, GDC-0152, and nec-1; or TNF, GDC-0152, Z-VAD, and nec-1 for 8 h. *g*, stable Neg, XIAP-G1, and XIAP-G2 iBMDM cell lines stimulated with either LPS; LPS and GDC-0152; LPS, GDC-0152, and Z-VAD; LPS, GDC-0152, and nec-1; or LPS, GDC-0152, Z-VAD, and nec-1 for 20–24 h were stained and quantified with methylene blue. *, $p \leq 0.05$ compared with the corresponding Neg treatment. *h*, Western blots analyzing lysates from Neg, XIAP-G1, and XIAP-G2 iBMDM stable cell lines treated for 8 h with either LPS; LPS and GDC-0152; LPS, GDC-0152, and Z-VAD; LPS, GDC-0152, and nec-1; or LPS, GDC-0152, Z-VAD, and nec-1. All Western blot experiments were performed three independent times. *a*–*d*, TNF (10 ng/ml), LPS (100 ng/ml), GDC-0152 (2 μM), nec-1 (20 μM), and Z-VAD (20 μM). *e*–*h*, TNF (10 ng/ml), LPS (100 ng/ml), GDC-0152 (200 nM), nec-1 (20 μM), and Z-VAD (20 μM). *FL*, full-length caspase-3; *CD*, cleaved caspase-3. All statistical analyses were performed using two-way ANOVA.

Reconstitution of XIAP-null stable cell lines with patient-derived XIAP variants

Given that loss of XIAP led to a combined NOD2 and cell death phenotype, we next wanted to determine whether patient-derived mutations exhibited a defect in NOD2, a lack of inhibition of cell death, or both of these phenotypes. To test this, we reconstituted WT XIAP, ubiquitin ligase-dead XIAP, or a disease-associated XIAP variant to the XIAP-null cell lines using a lentiviral construct recently developed by our laboratory (50). XIAP contains three BIR domains, an ubiquitin-binding domain, and a RING domain. Missense and nonsense mutations reported in the literature from patients with inflammatory disease were chosen for study that span the protein-coding sequence of XIAP and inserted with an N-terminal myc tag downstream of an antibiotic resistance gene in the lentiviral construct (Fig. 5*a*). To prevent residual CRISPR/Cas9 activity in the knockout cell lines from silencing the reconstitution lentiviral XIAP expression system, the NGG that is the protospacer-adjacent motif (PAM) of the sgRNA was mutated utilizing the degeneracy of the codons to conserve the amino acid at that position. As an intact NGG, PAM is required for Cas9 to generate a double-stranded break; mutation of the NGG prevents any residual CRISPR/Cas9 still present in the stable knockout cell lines from disrupting the reconstitution expression construct. The PAM of sgRNA-2 was mutated for the HEK293Ts (XIAP-G2), and the PAM of sgRNA-1 was mutated for the DC2.4s and iBMDMs (XIAP-G1). Following production of lentivirus, infection, and antibiotic selection, XIAP and associated mutants could be detected by antibodies directed to XIAP or the N-terminal myc tag in the whole-cell lysates at near endogenous levels of XIAP expression in HEK293Ts, DC2.4s, and iBMDMs (Fig. 5*b*). The myc tag was utilized to visualize the E99*X* and R381*X* mutants, as the epitope the XIAP monoclonal antibody recognizes is not sufficiently present in these two truncation mutants (Fig. 5, *a* and *b*).

After generating cell lines stably expressing XIAP or XIAP variant from a patient with inflammatory disease, we examined whether the XIAP variants exhibited a NOD2 defect. To test whether all generated XIAP mutants impair NOD2 activation, NF-κB luciferase assays were performed in the stably reconstituted XIAP HEK293T lines. NOD2 was overexpressed in the presence of a NF-κB-driven luciferase in each of the HEK293T reconstitution cell lines. Reconstitution of the XIAP-null HEK293T cells with WT XIAP restored NOD2-activated NF-κB-driven luciferase activity, indicating that XIAP reconstituted using the lentiviral construct is functional and capable of restoring XIAP activity at the NOD2 complex. Strikingly similar to WT XIAP, both G39C and K297T induced significantly greater NF-κB-driven luciferase activity relative to the empty vector reconstitution line. In contrast, the ubiquitin ligase-dead XIAP (H467A), all the nonsense mutations (E99*X*, R381*X*, and G466*X*), and both mutations to the BIR2 domain

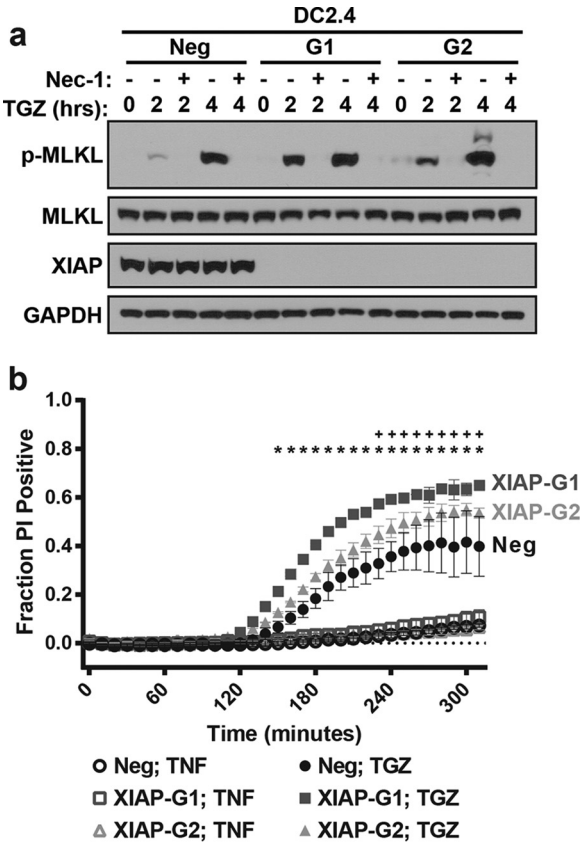

Figure 4. XIAP deletion leads to early necroptosis in dendritic cells. *a*, Western blot of lysates from DC2.4 Neg, XIAP-G1, and XIAP-G2 cell lines stimulated with TNF (10 ng/μl), GDC-0152 (2 μM), and Z-VAD (20 μM, *TGZ*) for 0, 2, or 4 h in the presence (+) or absence (−) of nec-1 (20 μM). Shown are representative blots from three independent replicates. *b*, 540-nm-stimulated 620-nm emission of DC2.4 Neg, XIAP-G1, and XIAP-G2 cell lines stimulated with TNF (10 ng/μl), GDC-0152 (2 μM), and Z-VAD (20 μM) in imaging medium containing propidium iodide (1 μg/ml). *, $p \leq 0.05$ Neg *versus* XIAP-G1; +, $p \leq 0.05$ Neg *versus* XIAP-G2 by two-way ANOVA.

(H220Y and C203Y) could not support NOD2 activation of NF-κB (Fig. 6*a*). Collectively, this provides evidence that not all XIAP mutations reported in patients with gastrointestinal inflammatory disease impair NOD2 function. Corroborating this finding, DC2.4 cells, similarly reconstituted, showed the same pattern of XIAP activity at the NOD2 complex in response to L18-MDP when assayed for expression of IRG1 by real-time quantitative PCR. XIAP, G39C, and K297T were all able to increase expression of IRG1 significantly above the empty reconstitution line, whereas the ligase-dead, nonsense, and BIR2 variants could not rescue NOD2 activity (Fig. 6*b*).

Given the prominent role of XIAP in restricting cell death and given that genetic loss of XIAP leads to both a NOD2 and a cell death phenotype, we next sought to examine whether the same set of XIAP variants exhibited a cell death phenotype. DC2.4 and iBMDM XIAP knockout cells stably reconstituted with either empty vector, wild-type XIAP, ubiquitin ligase-dead XIAP (H467A), or a disease-associated mutant were stimulated with either TNF or LPS with and without GDC-0152. Surprisingly, each XIAP variant that had a blunted NOD2 response (Fig. 6, *a* and *b*); H467A, E99*X*, R381*X*, G466*X*, H220Y, and C203Y also exhibited a profound inability to suppress both TNF- and LPS-driven cell death (Fig. 6, *c* and *d*). Similarly, all XIAP variants that restored NOD2 function also restored XIAP suppression of TNF- and LPS-induced cell death.

Although all variants that had a NOD2 defect also had a cell death defect, this does not rule out the possibility that a given XIAP variant alters the mechanism of cell death, being permissive to some but not other cell death pathways. To test whether the XIAP variants altered the mechanism of cell death compared with genetic loss of XIAP, reconstituted DC2.4s and iBMDMs were treated with TNF or LPS with and without GDC-0152 in combination with Z-VAD and nec-1. The XIAP variants with a greater sensitivity to cell death (H467A, E99*X*, R381*X*, G466*X*, H220Y, and C203Y) all mirrored the activity of their respective XIAP knockout cell lines, indicating that the variants do not alter the mechanism of cell death, but instead lower the threshold for activation of cell death (supplemental Fig. 1). These data represent the first isogenic examination of patient-derived XIAP variants that span the complete coding sequence. Importantly, it demonstrates that the NOD2 and cell death phenotype associated with patient-derived XIAP variants are inseparable. Specifically, patient-derived variants that have loss of function at the NOD2 complex also cannot inhibit cell death.

Prediction of XIAP activity for patient-directed insight

Selecting XIAP variants spanning the entire protein-coding sequence for study allowed us to begin addressing the difficult problem of predicting the cellular phenotype associated with XIAP variation. Our above data showed that, although five XIAP mutations reported in patients with inflammatory disease showed a strong cellular phenotype, two (G39C and K297T) did not. This finding suggests an important clinical feature highlighted by exome sequences: human genetic alterations are more common than previously realized (61). Although finding a sequence that differs from a reference sequence does not inherently mean that particular genetic change is driving disease, these discrepancies represent promising avenues of pursuit. Indeed, the data generated here utilizing variants discovered by this method generates a model to predict and test for deleterious mutations in patients. Specifically, we hypothesized that two separate predictions were possible. First, that we could predict *de novo* whether a XIAP variant would have WT or LOF activity at the NOD2 complex, and, second, when the MDP-driven NOD2 response was known, whether that variant would exhibit a cell death defect. To test this possibility, we identified a second set of three XIAP mutations in patients presenting with early-onset inflammatory disease (S253*X*, 868_869insT, and A321G) (Fig. 7*a*). Our model predicts that the nonsense mutation (S253*X*) and the insertion (868_869insT, leading to a frameshift and early stop codon) would behave as LOF variants both at the NOD2 complex and at inhibiting cell death, whereas the missense mutation, A321G, located in the third BIR domain, would retain WT function. To begin, PBMCs from patients harboring these mutations were gated for granulocytes, monocytes, and CD3+ T cells and analyzed for expression of XIAP by flow cytometry; Fig. 7*b* illustrates results from the granulocyte fraction, whereas supplemental Fig. 2 shows the granulocyte, CD3+ T cell, and

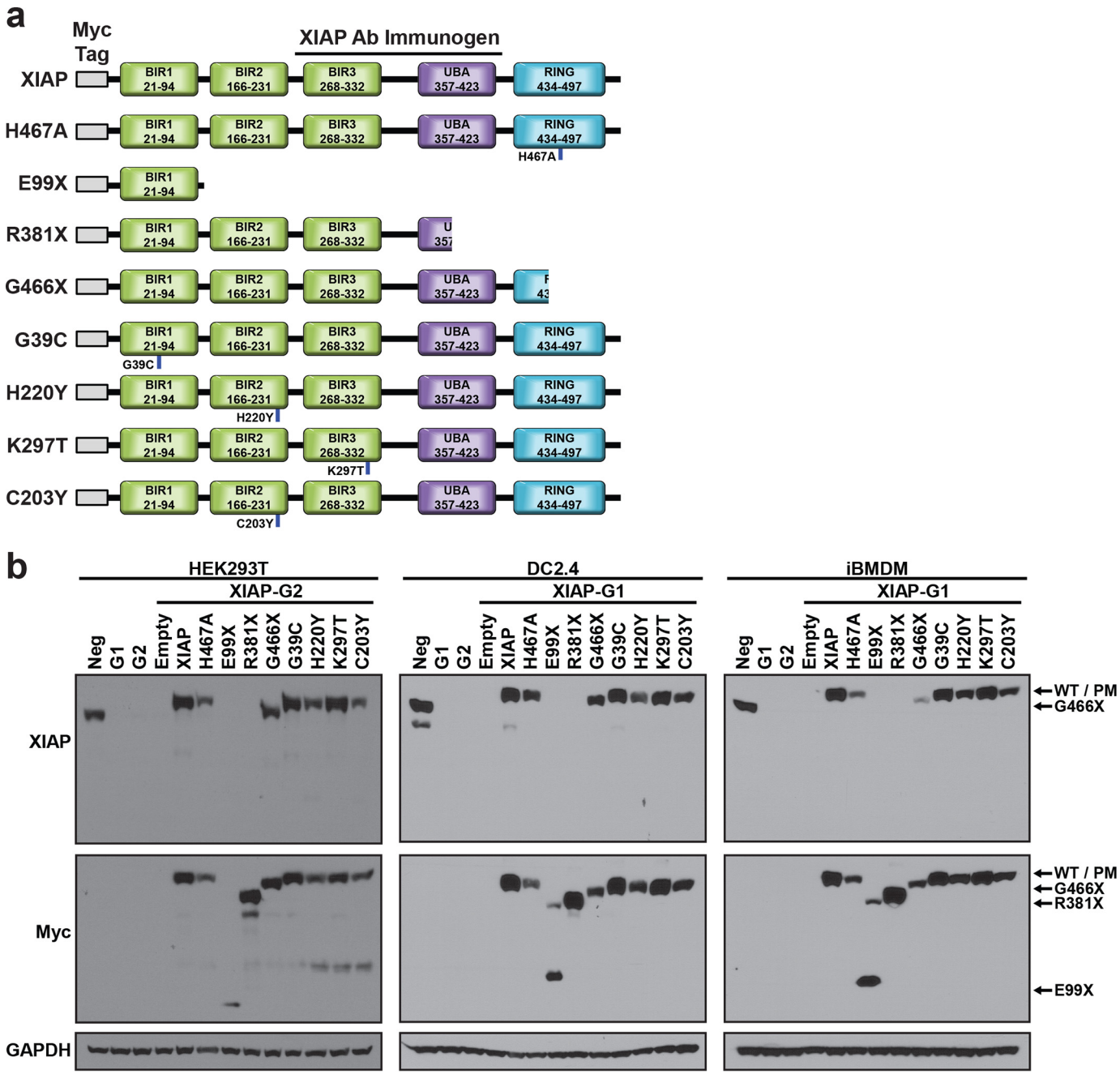

Figure 5. Reconstitution of XIAP-deficient cells with disease-associated XIAP variants. *a*, schematic of wild-type XIAP, ligase-dead XIAP (H467A), and seven disease-associated mutations (E99*X*, R381*X*, G4466*X*, G39C, C203Y, H220Y, and K297T) reconstituted to stable XIAP knockout lines. *b*, Western blots of the indicated stable XIAP knockout cell lines (HEK293T, DC2.4, and iBMDM) reconstituted with empty vector (*Empty*) or a variant of XIAP shown in *a* using a hygromycin-selectable (HEK293T) or puromycin-selectable (DC2.4 and iBMDM) lentiviral construct. In the *top blots*, no band for E99*X* and R381*X* is present, as they do not contain an adequate epitope for the anti-XIAP antibody. Expression of E99*X* and R381*X* can be visualized (along with all other variants) in the *center blots* via the N-terminal myc tag. *Arrows* indicate the expected locations of the different mutants. *PM*, point mutant.

monocyte XIAP expression data. Primary granulocytes from both patients with early stop codon mutations exhibited no significant XIAP signal over the isotype control, whereas the A321G cells exhibited XIAP expression comparable with a healthy donor control (Fig. 7*b* and supplemental Fig. 2).

As a first test to determine whether these variants exhibit a defect in activating NOD2, XIAP knockout DC2.4 dendritic cells reconstituted with S253X, 868_869insT, and A321G were stimulated as before with L18-MDP, and IRG1 expression was analyzed. Matching the prediction, S253*X* and 868_869insT failed to facilitate NOD2-induced expression of IRG1, and A321G induced IRG1 expression at wild-type levels (Fig. 7*c*). To confirm the endogenous NOD2 activity of these XIAP variants and to confirm the work done in cell lines, primary PBMCs from the patient harboring XIAP variant S253*X*, the patient harboring XIAP variant 868_869insT, and the patient harboring XIAP variant A321G were assayed for their capacity to induce IRG1 expression in response to L18-MDP stimulation. Corroborating the data seen in the cell lines, following L18-MDP stimulation for 2 h, PMBCs harboring XIAP variant

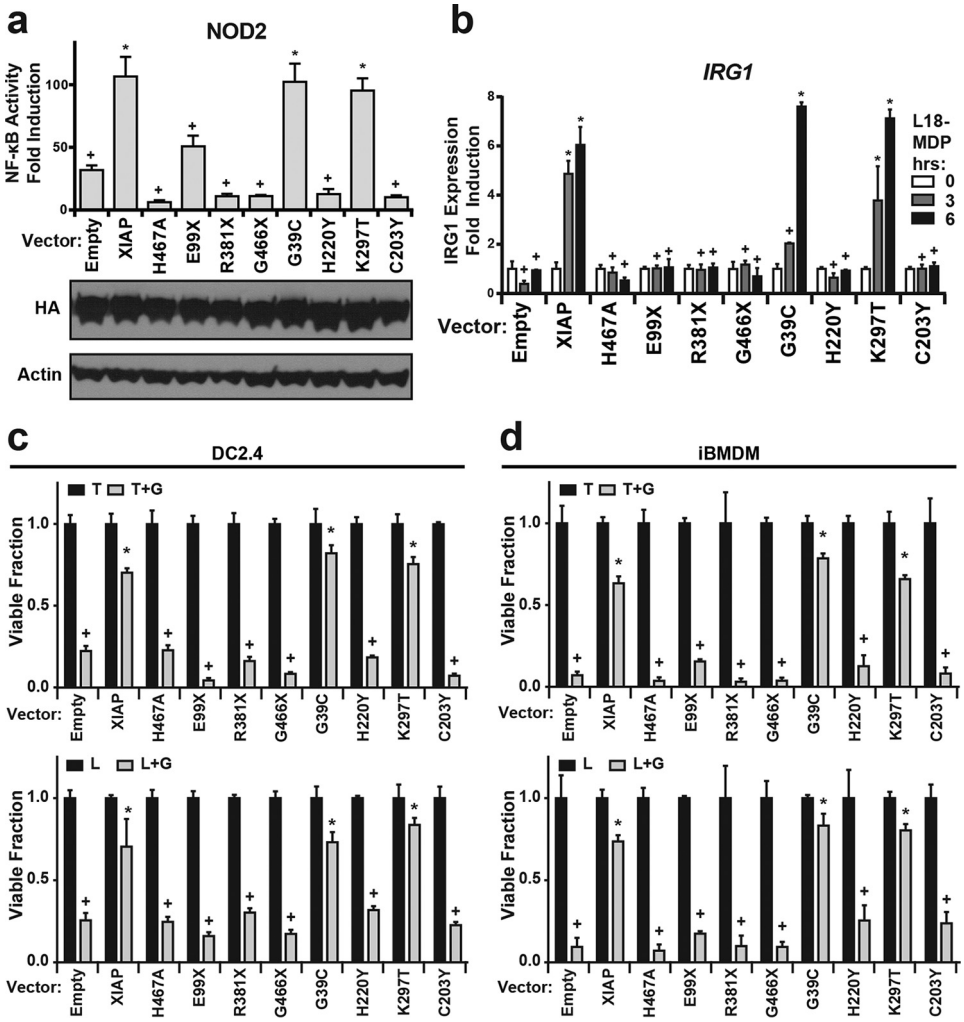

Figure 6. XIAP variants exhibit a combined NOD2 and cell death phenotype. *a*, *top panel*, NOD2-activated NF-κB luciferase assay in HEK293T cell lines reconstituted with variants of XIAP. *Bottom panel*, Western blots from a single replicate of the NF-κB luciferase assay above, evidencing equal transfection efficiency for the HA-tagged NOD2 used to induce NF-κB activity. *, $p \leq 0.05$ compared with Neg; +, $p \leq 0.05$ compared with XIAP. *b*, quantitative real-time PCR performed for IRG1 expression on DC2.4 cells stably expressing XIAP or a disease-associated variant stimulated with 10 μg/ml L18-MDP for 0, 3, or 6 h. *, $p \leq 0.05$ compared with the corresponding Neg time point; +, $p \leq 0.05$ compared with the corresponding XIAP time point by two-way ANOVA. *c*, the DC2.4 XIAP-G1 cell line stably reconstituted with empty vector or the XIAP variant (Fig. 5*a*) were stimulated with TNF in the presence (*T*+*G*) or absence (*T*) of GDC-0152 or LPS in the presence (*L*+*G*) or absence (*L*) of GDC-0152 for 20–24 h and subsequently stained with methylene blue and quantified (TNF, 10 ng/ml; LPS, 100 ng/ml; GDC-0152, 2 μM). *, $p \leq 0.05$ compared with the corresponding Neg treatment; +, $p \leq 0.05$ compared with the corresponding XIAP treatment by two-way ANOVA. *d*, as in *c*. iBMDM cell lines stably reconstituted with XIAP variant (Fig. 5*a*) were stimulated with TNF in the presence or absence of GDC-0152 or LPS in the presence or absence of GDC-0152 for 20–24 h, stained with methylene blue, and quantified. TNF, 10 ng/ml; LPS, 100 ng/ml; GDC-0152, 200 nM. *, $p \leq 0.05$ compared with the corresponding Neg treatment; +, $p \leq 0.05$ compared with the corresponding XIAP treatment by two-way ANOVA.

A321G facilitated NOD2-induced expression of IRG1 to a significantly higher level than those harboring either S253*X* or 868_869insT, and cells from patients harboring S253*X* and 868_869insT mutations failed to induce expression of IRG1 significantly above unstimulated cells following L18-MDP treatment (Fig. 7*d*).

Given that every XIAP variant we have tested to date with a NOD2 phenotype also has a cell death phenotype, we predicted that variants S253*X* and 868_869insT would be unable to suppress cell death, whereas A321G, which had WT function at the NOD2 complex, would readily suppress TNF- and LPS-induced cell death. To test this, XIAP knockout DC2.4 cells reconstituted with S253*X*, 868_869insT, and A321G were stimulated as before with either TNF or LPS with or without GDC-0152, and cell viability was determined. As predicted, S253*X* and 868_869insT were incapable of limiting TNF- or LPS-driven cell death, whereas A321G exhibited WT levels of cell death inhibition (Fig. 7*e*). This same pattern was identified in macrophages reconstituted with the new XIAP variants. S253*X* and 868_869insT showed significantly greater cell death, and A321G prevented cell death as efficiently as wild-type XIAP (Fig. 7*f*). Interestingly, as was seen for the first set of variants studied, NOD2 activation positively correlated with the capacity of a variant to restrict cell death. Specifically, every XIAP variant that behaved as having loss of function at the NOD2 complex also displayed a marked inability to suppress TNF- and LPS-induced cell death. Further, these data demonstrate that not every XIAP variant discovered to date has a detectable functional deficit, and means to predict and test XIAP variants for functional activity may likely improve our capacity to provide care by identifying patients carrying true LOF XIAP variants.

a

Genotype	Protein Expression Level	Phenotype Prediction	MDP Response	Cytotoxicity Response
S253X	Not Detected	Loss of Function	Loss of Function	Loss of Function
868_869insT	Not Detected	Loss of Function	Loss of Function	Loss of Function
A321G	Normal Expression	Wild-type Function	Wild-type Function	Wild-type Function

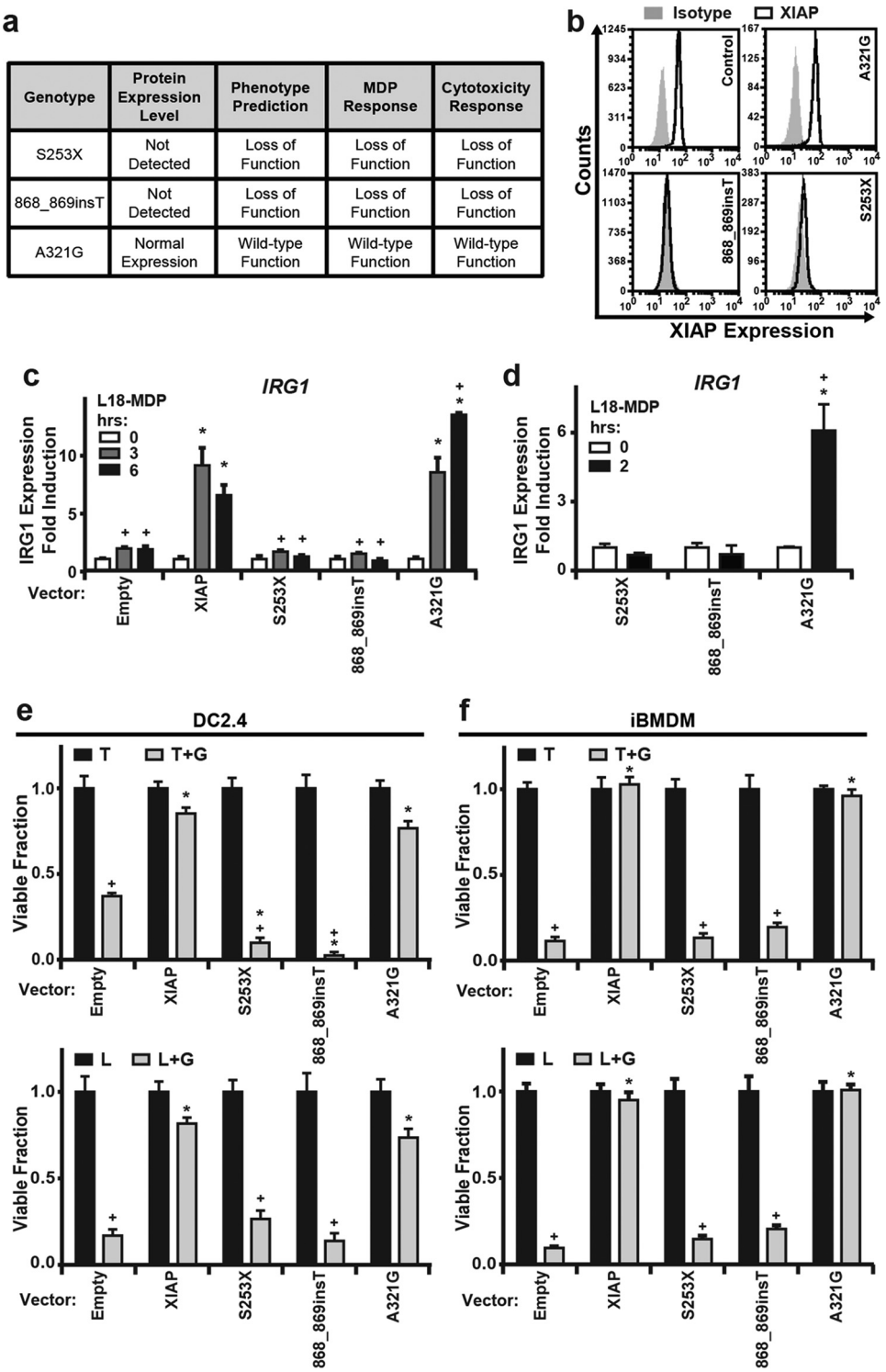

Figure 7. A novel set of patient-derived XIAP mutations and primary patient-derived PBMCs facilitates prediction of cell death and NOD2 defects. *a*, novel patient mutations used to test the capacity to predict cellular phenotype and patient PBMC response. *b*, flow plot histograms (counts on the *y* axis) of granulocytes, gated by forward and side scatter, analyzed for expression of XIAP (*x* axis). XIAP expression by flow cytometry for monocytes and CD3+ T cells can be found in supplemental Fig. 2. *c*, stable DC2.4 cells reconstituted with the novel XIAP variants in *a* were stimulated with L18-MDP (10 μg/ml) for 0, 3, and 6 h, and real-time PCR was performed for the expression of IRG1. *, $p \leq 0.05$ compared with the corresponding Neg time point; +, $p \leq 0.05$ compared with the corresponding XIAP time point by two-way ANOVA. *d*, quantitative PCR analysis of IRG1 expression of primary PBMCs from patients harboring S253*X*, 868_869insT, and A321G XIAP mutations following L18-MDP (10 μg/ml) stimulation for 0 or 2 h. *, $p \leq 0.05$ A321G *versus* S253*X*; +, $p \leq 0.05$ A321G *versus* 868_869insT for 2-h treatment by two-way ANOVA. *e*, quantification of viable cells by methylene blue staining of DC2.4 reconstituted with XIAP or variants from *a* stimulated with TNF (*T*) or TNF and GDC-0152 (*T*+*G*) (*top panel*) or LPS (*L*) or LPS and GDC-0152 (*L*+*G*) (*bottom panel*). *, $p \leq 0.05$ compared with Neg treatment; +, $p \leq 0.05$ compared with XIAP treatment by two-way ANOVA. *f*, viable fraction of iBMDM cell lines, reconstituted XIAP, or variants from *a* following stimulation with TNF in the absence (*T*) or presence (*T*+*G*) of GDC-0152 (*top panel*) and LPS (*L*) or LPS and GDC-0152 (*L*+*G*) (*bottom panel*). *, $p \leq 0.05$ compared with the corresponding Neg treatment; +, $p \leq 0.05$ compared with the corresponding XIAP treatment by two-way ANOVA.

Discussion

XIAP is known to be required for NOD2 signaling and known to limit cell death (15, 16, 20, 42, 43). Remarkably, its mutation leads to two major distinct clinical presentations: XLP-2, a disease characterized by life-threatening exaggerated cytokine responses to Epstein-Barr virus, and VEO-IBD, a severe, difficult-to-treat form of inflammatory bowel disease (17, 18, 62, 63). Given that loss-of-function NOD2 polymorphisms predispose to the development of Crohn's disease (reviewed in Ref. 7), it is attractive to attribute the totality of the role of XIAP in VEO-IBD to NOD2 dysfunction. Despite this, the clinical pathophysiology suggests that XIAP-driven inflammatory disease is not solely due to defective NOD signaling. Patients harboring XIAP mutations and those harboring NOD2 mutations that exhibit loss of function do not share the full complement of clinical symptoms. Patients with LOF NOD2 polymorphisms typically develop ileal Crohn's disease at a much later age (2–4, 7), whereas patients with XIAP mutations develop a severe pan-gastrointestinal tract inflammatory disease at an early age (18, 39). Additionally, patients who are compound-heterozygous for NOD2 polymorphisms show a much lower prevalence of disease than those who are hemizygous for XIAP mutations (39, 64, 65). Last, although the same mutations in XIAP can cause either IBD or XLP-2, there have been no reports of patients with NOD2 polymorphisms developing symptoms consistent with a comorbid diagnosis of XLP-2 or hemophagocytic lymphohistiocytosis. Given these discrepancies in clinical presentation, it is likely that XIAP-induced alterations in cell death pathways also contribute to XIAP-driven inflammatory disease.

Although cell death has been studied using XIAP-mutant patient cells, published results have been limited to T cells and intestinal epithelial cells and have been inconsistent (18, 39–41, 62). Depending on the study, there has either been no effect of XIAP mutation on T cell apoptosis (40), a substantial effect on T cell apoptosis (18), or a variable T cell apoptosis response not reconcilable with the nature of the mutations (62). In a single study using patient-derived tissue, no increased apoptosis was seen in intestinal epithelial cells with a markedly variable T cell apoptosis response (39), whereas another study using an XIAP-null immortalized colon cancer line found a variable epithelial cell defect partially protected by XIAP variants derived from patients (41). Patient-derived cells and patient-derived mutations have consistently shown a NOD2 signaling defect (18, 39–41), but study of the effect on cell death has been complicated by differing cell types, differing stimuli used, differing experimental readouts, and potentially by differing patient disease courses and treatments. Complicating this is the fact that the cell lines studied have not been those most responsive to either NOD2 stimuli or to inflammatory cell death. NOD2 is constitutively expressed in the macrophage/dendritic cell lineage, and these cells are the most responsive to initial stimulation with MDP (44–46). XIAP loss has been shown to sensitize macrophages to inflammatory cell death (42, 43), and it has now been shown that hematopoietic stem cell transplant is often the most effective long-term treatment for XIAP-driven inflammatory diseases (18, 47–49). Despite this, there has yet to be a study examining XIAP mutant-directed cell death in either macrophages or dendritic cells. In addition, examination of the functional activity of XIAP mutations that result in a truncated protein product is problematic in patient-derived primary PBMCs and tissue. This is due to the fact that the primary method of detection, flow cytometry using a monoclonal antibody to a C-terminal fragment of XIAP (62, 66), cannot detect truncated proteins when they are expressed. In this manuscript, we address these issues by generating XIAP-deficient macrophage and dendritic cell lines that not only show loss of XIAP expression but also loss of effective NOD2-dependent signaling (Fig. 1). We show that these cells are susceptible to inflammatory cell death in response to either TNF or LPS (Fig. 2), and we show that this preferentially occurs through apoptosis in macrophages and through combined apoptosis and necroptosis in dendritic cells (Figs. 3 and 4). We then use this novel system to reconstitute XLP-2 and VEO-IBD XIAP mutants at endogenous levels in these cell types, including truncation products that are difficult to detect clinically (Fig. 5). Using the cell lines reconstituted with patient-derived XIAP variants, we then show that mutants that lack the ability to signal through NOD2 also show increased susceptibility to inflammatory cell death (Fig. 6 and supplemental Fig. 1). Using this system, we then characterize three novel XLP-2 XIAP mutations and show that they have the same phenotype as those studied previously (Fig. 7). In all, this work helps to systematically study the role of patient-derived XIAP mutations in NOD2 signaling and in inflammation-related cell death susceptibility in the myeloid lineage, providing a framework and reagents for rapid testing of novel XIAP variants discovered in patients. This work shows that NOD2 signaling loss is linked to inflammatory cell death susceptibility through XIAP and not only develops a molecular framework for the study of novel XIAP mutations but also implies that inflammatory cell death is central to both XLP-2 and VEO-IBD pathogenesis.

Experimental procedures

Cells, plasmids, reagents, antibodies, and Western blotting

HEK293T cells used for virus production, and luciferase assays were purchased from the ATCC and cultured in DMEM (Corning) supplemented with 10% GemCell super calf serum (Gemini) and 1% antibiotics and 1% antimycotics (1% anti-anti, Gibco). Immortalized murine bone marrow-derived macrophages, originally from Dr. Eicke Latz (University of Bonn, Institute of Innate Immunity) were cultured as described previously (67). The dendritic cell line DC2.4 was obtained under an approved material transfer agreement from Dr. Kenneth Rock (University of Massachusetts Medical School, Department of Pathology, Worcester, MA) and cultured in RPMI (Corning) supplemented with 10% heat-inactivated super calf serum, 1% antibiotics and 1% antimycotics (1% anti-anti, Gibco), 2 mM L-glutamine (Gibco), 1× MEM nonessential amino acids (Gibco), 1 mM HEPES (pH 7.4) (Fisher Scientific), and 50 μM 2-mercaptoethanol (Fisher).

pEBB-XIAP (38) was a gift from Jon Ashwell (Addgene plasmid 11558). pMD2.G (Addgene plasmid 12259) and PsPax2 (Addgene plasmid 12260) were a gift from Didier Trono. Len-

tiCrispV2 (51) was a gift from Feng Zhang (Addgene plasmid 52961). pcDNA3-HA-NOD1 and pcDNA3-HA-NOD2 were a generous gift from Dr. Christine McDonald (Department of Pathology, Cleveland Clinic Foundation, Cleveland, OH). Generation of stable XIAP-expressing reconstitution cell lines was achieved using a novel lentiviral vector we developed recently (50). To increase the range of use of the LentiCrisprV2 with our reconstitution construct, the original puromycin resistance gene was replaced with the hygromycin resistance gene, yielding a new LentiCrisprV2 construct selectable with hygromycin. To generate mutations to XIAP-containing plasmids corresponding to genetic XIAP variants, site-directed mutagenesis was performed (Stratagene) using primers designed by an online tool. All new constructs generated, including the novel lentiviral construct containing XIAP and either a hygromycin or puromycin resistance gene, were constructed using Gibson double-stranded DNA isothermal assembly methods (68).

Proteins of interest were detected by Western blotting following lysis in complete Triton lysis buffer containing 150 mM NaCl, 50 mM Tris (pH 7.4), 2.5 mM sodium pyrophosphate, 1 mM β-glycerophosphate, 5 mM iodoacetamide, 5 mM *N*-ethylmaleimide, 1 mM PMSF, 1 mM sodium orthovanadate, 1 mM EGTA, 1 mM EDTA, 1% Triton X-100, and complete protease inhibitor mixture (Sigma) using mouse monoclonal antibody to XIAP (BD Transduction Laboratories), mouse polyclonal antibody to GAPDH (ProteinTech), rabbit monoclonal antibody to phosphorylated MLKL (Abcam), rabbit polyclonal antibody to mouse MLKL (Abgent), mouse monoclonal antibody to the HA tag (BioLegend), goat polyclonal antibody to actin (Santa Cruz Biotechnology), rabbit monoclonal antibody to the myc tag (Cell Signaling Technology), and rabbit polyclonal antibody to caspase-3 (Cell Signaling Technology) and used according to the instructions of the manufacturer. HRP-conjugated antibodies recognizing mouse and rabbit IgG were from Cell Signaling Technology, and HRP-conjugated antibody recognizing goat IgG was purchased from Southern BioTech. Luciferase assays were performed on a Wallac Victor3V (PerkinElmer Life Sciences) using the Dual-Luciferase reporter kit from Promega.

CRISPR/SpCas9 knockout of XIAP and stable cell line generation

Generation of stable XIAP knockout cell lines was achieved using the LentiCrisprV2 system. Lentivirus was produced by calcium phosphate transfection of the lentiviral plasmid, pMD2.G, and PsPax2 in a 4 to 3 to 1.2 ratio to HEK293T cells. After 2 days of virus production, supernatants were harvested and cleared by centrifugation, followed by filtration through a 0.45-μm syringe filter. Recipient cells were then incubated in the cleared viral supernatants with Polybrene transfection reagent (EMD Millipore, 10 μg/ml) for 2 days. After transduction with lentivirus, cells were stably selected in either puromycin (Invivogen, 2 μg/ml, HEK293Ts) or hygromycin (Invivogen, 350 μg/ml, iBMDMs and DC2.4s), and single-cell clone populations were generated, expanded, and tested by Western blotting for expression of XIAP. Six or more individual clones with undetectable expression of XIAP were then pooled to generate stable knockout pools for each sgRNA.

A novel lentiviral vector generated recently in our laboratory was used to reconstitute XIAP or variant to the generated XIAP knockout lines. An EF1a promoter drives expression of a selectable marker coupled by a P2A self-cleaving peptide to a triply myc-tagged XIAP or variant. Infection of cells with this construct results in selectable expression of XIAP. The reconstitution construct contains either the puromycin resistance gene or the hygromycin resistance gene, depending on which LentiCrisprV2 construct was used. HEK293Ts received a puromycin-selectable LentiCrisprV2 and hygromycin-selectable reconstitution construct. DC2.4s and iBMDMs received a hygromycin-selectable LentiCrisprV2 and puromycin-selectable reconstitution construct. To prevent residually expressed CRISPR/SpCas9 in the parent knockout cell line from disrupting the reconstitution construct, the PAM was mutated, in the viral construct corresponding to the sgRNA of the stable knockout cell line being transformed, to a stable reconstitution cell line. Virus was produced as above, and after antibiotic selection for at least a week, the entire virally transduced and stably selected pool was used to assay expression and for experiments.

RNA and quantitative real-time PCR

Messenger RNA was isolated from cells using the QiaShredder and RNEasy kits (Qiagen, catalog nos. 79656 and 74136, respectively) and converted to cDNA using the Quantitect reverse transcription kit (Qiagen, catalog no. 205313) according to the instructions of the manufacturer. Real-time quantitative PCR was performed with iQ SYBR Green Supermix (Bio-Rad, catalog no. 170-8882) using primers to GAPDH (human, 5′-CTCCTGTTCGACAGTCAGCC-3′ (forward) and 5′-CGACCAAATCCGTTGACTCC-3′] (reverse); mouse, 5′-AGGCCGGTGCTGAGTATGTC-3′ (forward) and 5′-TGCCTGCTTCACCACCTTCT-3′] (reverse)) and IRG1 (human, 5′-CAAGGAGGCCAATGACATGC-3′ (forward) and 5′-AGCTTCTCGGCACTTTGTCG-3′ (reverse); mouse, 5′-GTTTGGGGTCGACCAGACTT-3′ (forward) and 5′-CAGGTCGAGGCCAGAAAACT-3′ (reverse)) on a Bio-Rad CFX96 C1000 real-time thermocycler system. Experiments were performed in technical duplicates three times. For quantitative real-time PCR on PBMCs isolated from patients, whole viable PBMCs of a given genetic background (*e.g.* A321G, S253*X*, or 868_869insT) were stimulated in three (A321G and 868_869insT) or two (S253*X*) separate experiments. Each of these replicates were performed on separate days.

TNF and LPS cytotoxicity assays

The day before starting treatment, cells were plated at 200,000–300,000 cells/well in a 24-well plate (Corning). The following day, the medium was changed to contain the indicated treatment with LPS (Invivogen), GDC-0152 (MedChem Express), necrostatin-1 (Apex Bio), and Z-VAD (Apex Bio). The recombinant TNF used in these studies was from Gold Biotechnology or was purified by a GST tag from bacterial expression, and LPS was removed by Pierce high-capacity endotoxin removal resin (Thermo Fisher Scientific). For LPS cytotoxicity studies, cells were pretreated with LPS for 3–4 h prior to treatment. Following 18–24 h of treatment, 24-well

plates were washed once in PBS (135 mM NaCl, 2.7 mM KCl, 10 mM Na_2HPO_4, and 1.8 mM KH_2PO_4 (pH 7.4)) and incubated for 10 min with 0.2 μM sterile filtered ice-cold methylene blue (Sigma, 2 g/ml) mixed in a 1:1 solution of methanol and distilled water. After washing twice with PBS, stained plates were air-dried and scanned at 1200 dots per inch in 24-bit true color on a Brother MFC-J4510DW. Individual wells of the 24-well plates were then quantified using ImageJ (National Institutes of Health, Bethesda, MD) for the presence of retained methylene blue in each well.

Propidium iodide influx assays

The day before the experiment cells were plated at 500,000 cells per well in a 24-well plate (Corning) and allowed to adhere overnight. On the day of the experiment, immediately before taking fluorescent measurements, the medium was changed to a filter-sterilized balanced salt solution (130 mM NaCl, 4 mM KCl, 1.5 mM $CaCl_2$,1 mM $MgCl_2$, 25 mM sodium HEPES, and 5 mM D-glucose (pH 7.4)) supplemented with 0.1% BSA and 1 μg/ml propidium iodide. Using a BioTek Synergy HT plate reader heated to 37 °C, 620-nm emission following 540-nm excitation was recorded at 10-min intervals. After a brief period to record background fluorescence, cells were stimulated with TNF (10 ng/ml) or TNF (10 ng/ml), GDC-0152 (2 μM), and Z-VAD (20 μM) to induce necroptosis.

Acquisition of patient PBMCs and flow cytometric detection of XIAP

Patients consented to a Cincinnati Children's Hospital Institutional Review Board approved protocol. Peripheral blood mononuclear cells were isolated from peripheral blood samples by density gradient centrifugation. Sequencing and measurement of XIAP by flow cytometry was performed as reported previously (66).

Author contributions—S. M. C. designed and performed experiments, interpreted data from all experiments, and wrote the manuscript. R. A. M. provided sequencing, expression data, and primary patient PBMCs and edited the manuscript. P. K. performed experiments. J. K. R. generated cell lines and performed experiments. G. R. D. designed and aided in performing propidium iodide influx assays, interpreted data, and edited the manuscript. D. W. A. conceived the project, designed experiments, interpreted the data from all experiments, and wrote the manuscript.

Acknowledgments—We thank Tsan Xiao and Jie Yang for purification of GST-TNF and Parameswaran Ramakrishnan, Fabio Cominelli, Christine McDonald, Xiaoxia Li, and Theresa Pizarro for critical conversations and critiques of the manuscript.

References

1. Hugot, J. P., Laurent-Puig, P., Gower-Rousseau, C., Olson, J. M., Lee, J. C., Beaugerie, L., Naom, I., Dupas, J. L., Van Gossum, A., Orholm, M., Bonaiti-Pellie, C., Weissenbach, J., Mathew, C. G., Lennard-Jones, J. E., Cortot, A., *et al.* (1996) Mapping of a susceptibility locus for Crohn's disease on chromosome 16. *Nature* **379,** 821–823
2. Hugot, J. P., Chamaillard, M., Zouali, H., Lesage, S., Cézard, J. P., Belaiche, J., Almer, S., Tysk, C., O'Morain, C. A., Gassull, M., Binder, V., Finkel, Y., Cortot, A., Modigliani, R., Laurent-Puig, P., *et al.* (2001) Association of NOD2 leucine-rich repeat variants with susceptibility to Crohn's disease. *Nature* **411,** 599–603
3. Ogura, Y., Bonen, D. K., Inohara, N., Nicolae, D. L., Chen, F. F., Ramos, R., Britton, H., Moran, T., Karaliuskas, R., Duerr, R. H., Achkar, J. P., Brant, S. R., Bayless, T. M., Kirschner, B. S., Hanauer, S. B., *et al.* (2001) A frameshift mutation in NOD2 associated with susceptibility to Crohn's disease. *Nature* **411,** 603–606
4. Hampe, J., Grebe, J., Nikolaus, S., Solberg, C., Croucher, P. J., Mascheretti, S., Jahnsen, J., Moum, B., Klump, B., Krawczak, M., Mirza, M. M., Foelsch, U. R., Vatn, M., and Schreiber, S. (2002) Association of NOD2 (CARD 15) genotype with clinical course of Crohn's disease: a cohort study. *Lancet* **359,** 1661–1665
5. Schürmann, M., Valentonyte, R., Hampe, J., Müller-Quernheim, J., Schwinger, E., and Schreiber, S. (2003) CARD15 gene mutations in sarcoidosis. *Eur. Respir. J.* **22,** 748–754
6. Kanazawa, N., Okafuji, I., Kambe, N., Nishikomori, R., Nakata-Hizume, M., Nagai, S., Fuji, A., Yuasa, T., Manki, A., Sakurai, Y., Nakajima, M., Kobayashi, H., Fujiwara, I., Tsutsumi, H., Utani, A., *et al.* (2005) Early-onset sarcoidosis and CARD15 mutations with constitutive nuclear factor-κB activation: common genetic etiology with Blau syndrome. *Blood* **105,** 1195–1197
7. Abraham, C., and Cho, J. H. (2006) Functional consequences of NOD2 (CARD15) mutations. *Inflamm. Bowel Dis.* **12,** 641–650
8. Negroni, A., Stronati, L., Pierdomenico, M., Tirindelli, D., Di Nardo, G., Mancini, V., Maiella, G., and Cucchiara, S. (2009) Activation of NOD2-mediated intestinal pathway in a pediatric population with Crohn's disease. *Inflamm. Bowel Dis.* **15,** 1145–1154
9. Shaw, P. J., Barr, M. J., Lukens, J. R., McGargill, M. A., Chi, H., Mak, T. W., and Kanneganti, T.-D. (2011) Signaling via the RIP2 adaptor protein in central nervous system-infiltrating dendritic cells promotes inflammation and autoimmunity. *Immunity* **34,** 75–84
10. Yao, Q., Zhou, L., Cusumano, P., Bose, N., Piliang, M., Jayakar, B., Su, L.-C., and Shen, B. (2011) A new category of autoinflammatory disease associated with NOD2 gene mutations. *Arthritis Res. Ther.* **13,** R148
11. Magalhaes, J. G., Fritz, J. H., Le Bourhis, L., Sellge, G., Travassos, L. H., Selvanantham, T., Girardin, S. E., Gommerman, J. L., and Philpott, D. J. (2008) Nod2-dependent Th2 polarization of antigen-specific immunity. *J. Immunol.* **181,** 7925–7935
12. Daley, D., Lemire, M., Akhabir, L., Chan-Yeung, M., He, J. Q., McDonald, T., Sandford, A., Stefanowicz, D., Tripp, B., Zamar, D., Bosse, Y., Ferretti, V., Montpetit, A., Tessier, M.-C., Becker, A., *et al.* (2009) Analyses of associations with asthma in four asthma population samples from Canada and Australia. *Hum. Genet.* **125,** 445–459
13. Duan, W., Mehta, A. K., Magalhaes, J. G., Ziegler, S. F., Dong, C., Philpott, D. J., and Croft, M. (2010) Innate signals from Nod2 block respiratory tolerance and program TH2-driven allergic inflammation. *J. Allergy Clin. Immunol.* **126,** 1284–1293.e10
14. Tigno-Aranjuez, J. T., and Abbott, D. W. (2012) Ubiquitination and phosphorylation in the regulation of NOD2 signaling and NOD2-mediated disease. *Biochim. Biophys. Acta* **1823,** 2022–2028
15. Krieg, A., Correa, R. G., Garrison, J. B., Le Negrate, G., Welsh, K., Huang, Z., Knoefel, W. T., and Reed, J. C. (2009) XIAP mediates NOD signaling via interaction with RIP2. *Proc. Natl. Acad. Sci.* **106,** 14524–14529
16. Damgaard, R. B., Nachbur, U., Yabal, M., Wong, W. W., Fiil, B. K., Kastirr, M., Rieser, E., Rickard, J. A., Bankovacki, A., Peschel, C., Ruland, J., Bekker-Jensen, S., Mailand, N., Kaufmann, T., Strasser, A., *et al.* (2012) The ubiquitin ligase XIAP recruits LUBAC for NOD2 signaling in inflammation and innate immunity. *Mol. Cell.* **46,** 746–758
17. Rigaud, S., Fondanèche, M.-C., Lambert, N., Pasquier, B., Mateo, V., Soulas, P., Galicier, L., Le Deist, F., Rieux-Laucat, F., Revy, P., Fischer, A., de Saint Basile, G., and Latour, S. (2006) XIAP deficiency in humans causes an X-linked lymphoproliferative syndrome. *Nature* **444,** 110–114
18. Worthey, E. A., Mayer, A. N., Syverson, G. D., Helbling, D., Bonacci, B. B., Decker, B., Serpe, J. M., Dasu, T., Tschannen, M. R., Veith, R. L., Basehore, M. J., Broeckel, U., Tomita-Mitchell, A., Arca, M. J., Casper, J. T., *et al.* (2011) Making a definitive diagnosis: successful clinical application of whole exome sequencing in a child with intractable inflammatory bowel disease. *Genet. Med.* **13,** 255–262

19. Galbán, S., and Duckett, C. S. (2010) XIAP as a ubiquitin ligase in cellular signaling. *Cell Death Differ.* **17,** 54–60
20. Deveraux, Q. L., Takahashi, R., Salvesen, G. S., and Reed, J. C. (1997) X-linked IAP is a direct inhibitor of cell-death proteases. *Nature* **388,** 300–304
21. Chai, J., Shiozaki, E., Srinivasula, S. M., Wu, Q., Datta, P., Alnemri, E. S., Shi, Y., and Dataa, P. (2001) Structural basis of caspase-7 inhibition by XIAP. *Cell* **104,** 769–780
22. Takahashi, R., Deveraux, Q., Tamm, I., Welsh, K., Assa-Munt, N., Salvesen, G. S., and Reed, J. C. (1998) A single BIR domain of XIAP sufficient for inhibiting caspases. *J. Biol. Chem.* **273,** 7787–7790
23. Riedl, S. J., Renatus, M., Schwarzenbacher, R., Zhou, Q., Sun, C., Fesik, S. W., Liddington, R. C., and Salvesen, G. S. (2001) Structural basis for the inhibition of caspase-3 by XIAP. *Cell* **104,** 791–800
24. Shiozaki, E. N., Chai, J., Rigotti, D. J., Riedl, S. J., Li, P., Srinivasula, S. M., Alnemri, E. S., Fairman, R., and Shi, Y. (2003) Mechanism of XIAP-mediated inhibition of caspase-9. *Mol. Cell* **11,** 519–527
25. Schile, A. J., García-Fernández, M., and Steller, H. (2008) Regulation of apoptosis by XIAP ubiquitin-ligase activity. *Genes Dev.* **22,** 2256–2266
26. Brady, G. F., Galbán, S., Liu, X., Basrur, V., Gitlin, J. D., Elenitoba-Johnson, K. S., Wilson, T. E., and Duckett, C. S. (2010) Regulation of the copper chaperone CCS by XIAP-mediated ubiquitination. *Mol. Cell. Biol.* **30,** 1923–1936
27. Mufti, A. R., Burstein, E., Csomos, R. A., Graf, P. C., Wilkinson, J. C., Dick, R. D., Challa, M., Son, J. K., Bratton, S. B., Su, G. L., Brewer, G. J., Jakob, U., and Duckett, C. S. (2006) XIAP is a copper binding protein deregulated in Wilson's disease and other copper toxicosis disorders. *Mol. Cell* **21,** 775–785
28. Burstein, E., Ganesh, L., Dick, R. D., van De Sluis, B., Wilkinson, J. C., Klomp, L. W., Wijmenga, C., Brewer, G. J., Nabel, G. J., and Duckett, C. S. (2004) A novel role for XIAP in copper homeostasis through regulation of MURR1. *EMBO J.* **23,** 244–254
29. Huang, X., Wu, Z., Mei, Y., and Wu, M. (2013) XIAP inhibits autophagy via XIAP-Mdm2-p53 signalling. *EMBO J.* **32,** 2204–2216
30. Schwerd, T., Pandey, S., Yang, H.-T., Bagola, K., Jameson, E., Jung, J., Lachmann, R. H., Shah, N., Patel, S. Y., Booth, C., Runz, H., Düker, G., Bettels, R., Rohrbach, M., Kugathasan, S., *et al.* (2016) Impaired antibacterial autophagy links granulomatous intestinal inflammation in Niemann-Pick disease type C1 and XIAP deficiency with NOD2 variants in Crohn's disease. *Gut* 10.1136/gutjnl-2015–310382
31. Hsieh, W.-C., Chuang, Y.-T., Chiang, I. H., Hsu, S.-C., Miaw, S.-C., and Lai, M.-Z. (2014) Inability to resolve specific infection generates innate immunodeficiency syndrome in Xiap$^{-/-}$ mice. *Blood* **124,** 2847–2857
32. Bauler, L. D., Duckett, C. S., and O'Riordan, M. X. (2008) XIAP regulates cytosol-specific innate immunity to *Listeria* infection. *PLoS Pathog.* **4,** e1000142
33. Prakash, H., Albrecht, M., Becker, D., Kuhlmann, T., and Rudel, T. (2010) Deficiency of XIAP leads to sensitization for *Chlamydophila pneumoniae* pulmonary infection and dysregulation of innate immune response in mice. *J. Biol. Chem.* **285,** 20291–20302
34. Sun, C., Cai, M., Gunasekera, A. H., Meadows, R. P., Wang, H., Chen, J., Zhang, H., Wu, W., Xu, N., Ng, S. C., and Fesik, S. W. (1999) NMR structure and mutagenesis of the inhibitor-of-apoptosis protein XIAP. *Nature* **401,** 818–822
35. Eckelman, B. P., Salvesen, G. S., and Scott, F. L. (2006) Human inhibitor of apoptosis proteins: why XIAP is the black sheep of the family. *EMBO Rep.* **7,** 988–994
36. Duckett, C. S., Nava, V. E., Gedrich, R. W., Clem, R. J., Van Dongen, J. L., Gilfillan, M. C., Shiels, H., Hardwick, J. M., and Thompson, C. B. (1996) A conserved family of cellular genes related to the baculovirus iap gene and encoding apoptosis inhibitors. *EMBO J.* **15,** 2685–2694
37. Gyrd-Hansen, M., Darding, M., Miasari, M., Santoro, M. M., Zender, L., Xue, W., Tenev, T., da Fonseca, P. C., Zvelebil, M., Bujnicki, J. M., Lowe, S., Silke, J., and Meier, P. (2008) IAPs contain an evolutionarily conserved ubiquitin-binding domain that regulates NF-κB as well as cell survival and oncogenesis. *Nat. Cell Biol.* **10,** 1309–1317
38. Yang, Y., Fang, S., Jensen, J. P., Weissman, A. M., and Ashwell, J. D. (2000) Ubiquitin protein ligase activity of IAPs and their degradation in proteasomes in response to apoptotic stimuli. *Science* **288,** 874–877
39. Aguilar, C., Lenoir, C., Lambert, N., Bègue, B., Brousse, N., Canioni, D., Berrebi, D., Roy, M., Gérart, S., Chapel, H., Schwerd, T., Siproudhis, L., Schäppi, M., Al-Ahmari, A., Mori, M., *et al.* (2014) Characterization of Crohn disease in X-linked inhibitor of apoptosis-deficient male patients and female symptomatic carriers. *J. Allergy Clin. Immunol.* **134,** 1131–1141.e9
40. Zeissig, Y., Petersen, B.-S., Milutinovic, S., Bosse, E., Mayr, G., Peuker, K., Hartwig, J., Keller, A., Kohl, M., Laass, M. W., Billmann-Born, S., Brandau, H., Feller, A. C., Röcken, C., Schrappe, M., *et al.* (2015) XIAP variants in male Crohn's disease. *Gut* **64,** 66–76
41. Damgaard, R. B., Fiil, B. K., Speckmann, C., Yabal, M., zur Stadt, U., Bekker-Jensen, S., Jost, P. J., Ehl, S., Mailand, N., and Gyrd-Hansen, M. (2013) Disease-causing mutations in the XIAP BIR2 domain impair NOD2-dependent immune signalling. *EMBO Mol. Med.* **5,** 1278–1295
42. Yabal, M., Müller, N., Adler, H., Knies, N., Groß, C. J., Damgaard, R. B., Kanegane, H., Ringelhan, M., Kaufmann, T., Heikenwälder, M., Strasser, A., Groß, O., Ruland, J., Peschel, C., Gyrd-Hansen, M., and Jost, P. J. (2014) XIAP restricts TNF- and RIP3-dependent cell death and inflammasome activation. *Cell Rep.* **7,** 1796–1808
43. Lawlor, K. E., Khan, N., Mildenhall, A., Gerlic, M., Croker, B. A., D'Cruz, A. A., Hall, C., Kaur Spall, S., Anderton, H., Masters, S. L., Rashidi, M., Wicks, I. P., Alexander, W. S., Mitsuuchi, Y., Benetatos, C. A., *et al.* (2015) RIPK3 promotes cell death and NLRP3 inflammasome activation in the absence of MLKL. *Nat. Commun.* **6,** 6282
44. Ogura, Y., Inohara, N., Benito, A., Chen, F. F., Yamaoka, S., and Nunez, G. (2001) Nod2, a Nod1/Apaf-1 family member that is restricted to monocytes and activates NF-κB. *J. Biol. Chem.* **276,** 4812–4818
45. Kobayashi, K. S., Chamaillard, M., Ogura, Y., Henegariu, O., Inohara, N., Nuñez, G., and Flavell, R. A. (2005) Nod2-dependent regulation of innate and adaptive immunity in the intestinal tract. *Science* **307,** 731–734
46. Gutierrez, O., Pipaon, C., Inohara, N., Fontalba, A., Ogura, Y., Prosper, F., Nunez, G., and Fernandez-Luna, J. L. (2002) Induction of Nod2 in myelomonocytic and intestinal epithelial cells via nuclear factor-κB activation. *J. Biol. Chem.* **277,** 41701–41705
47. Marsh, R. A., Rao, K., Satwani, P., Lehmberg, K., Müller, I., Li, D., Kim, M.-O., Fischer, A., Latour, S., Sedlacek, P., Barlogis, V., Hamamoto, K., Kanegane, H., Milanovich, S., Margolis, D. A., *et al.* (2013) Allogeneic hematopoietic cell transplantation for XIAP deficiency: an international survey reveals poor outcomes. *Blood* **121,** 877–883
48. Jiang, M. Y., Guo, X., Sun, S. W., Li, Q., and Zhu, Y. P. (2016) Successful allogeneic hematopoietic stem cell transplantation in a boy with X-linked inhibitor of apoptosis deficiency presenting with hemophagocytic lymphohistiocytosis: a case report. *Exp. Ther. Med.* **12,** 1341–1344
49. Tsuma, Y., Imamura, T., Ichise, E., Sakamoto, K., Ouchi, K., Osone, S., Ishida, H., Wada, T., and Hosoi, H. (2015) Successful treatment of idiopathic colitis related to XIAP deficiency with allo-HSCT using reduced-intensity conditioning. *Pediatr. Transplant.* **19,** E25-E28
50. Chirieleison, S. M., Kertesy, S. B., and Abbott, D. W. (2016) Synthetic biology reveals the uniqueness of the RIP kinase domain. *J. Immunol.* **196,** 4291–4297
51. Sanjana, N. E., Shalem, O., and Zhang, F. (2014) Improved vectors and genome-wide libraries for CRISPR screening. *Nat. Methods* **11,** 783–784
52. Tigno-Aranjuez, J. T., Benderitter, P., Rombouts, F., Deroose, F., Bai, X., Mattioli, B., Cominelli, F., Pizarro, T. T., Hoflack, J., and Abbott, D. W. (2014) *In vivo* inhibition of RIPK2 kinase alleviates inflammatory disease. *J. Biol. Chem.* **289,** 29651–29664
53. Huang, Y., Park, Y. C., Rich, R. L., Segal, D., Myszka, D. G., and Wu, H. (2001) Structural basis of caspase inhibition by XIAP differential roles of the linker versus the BIR domain. *Cell* **104,** 781–790
54. Flygare, J. A., Beresini, M., Budha, N., Chan, H., Chan, I. T., Cheeti, S., Cohen, F., Deshayes, K., Doerner, K., Eckhardt, S. G., Elliott, L. O., Feng, B., Franklin, M. C., Reisner, S. F., Gazzard, L., *et al.* (2012) Discovery of a potent small-molecule antagonist of inhibitor of apoptosis (IAP) proteins and clinical candidate for the treatment of cancer (GDC-0152). *J. Med. Chem.* **55,** 4101–4113

55. Varfolomeev, E., Blankenship, J. W., Wayson, S. M., Fedorova, A. V., Kayagaki, N., Garg, P., Zobel, K., Dynek, J. N., Elliott, L. O., Wallweber, H. J., Flygare, J. A., Fairbrother, W. J., Deshayes, K., Dixit, V. M., and Vucic, D. (2007) IAP antagonists induce autoubiquitination of c-IAPs, NF-κB activation, and TNFα-dependent apoptosis. *Cell* **131,** 669–681
56. Vince, J. E., Wong, W. W., Khan, N., Feltham, R., Chau, D., Ahmed, A. U., Benetatos, C. A., Chunduru, S. K., Condon, S. M., McKinlay, M., Brink, R., Leverkus, M., Tergaonkar, V., Schneider, P., Callus, B. A., *et al.* (2007) IAP antagonists target cIAP1 to induce TNFα-dependent apoptosis. *Cell* **131,** 682–693
57. Wang, H., Sun, L., Su, L., Rizo, J., Liu, L., Wang, L.-F., Wang, F.-S., and Wang, X. (2014) Mixed lineage kinase domain-like protein MLKL causes necrotic membrane disruption upon phosphorylation by RIP3. *Mol. Cell* **54,** 133–146
58. Holler, N., Zaru, R., Micheau, O., Thome, M., Attinger, A., Valitutti, S., Bodmer, J. L., Schneider, P., Seed, B., and Tschopp, J. (2000) Fas triggers an alternative, caspase-8-independent cell death pathway using the kinase RIP as effector molecule. *Nat. Immunol.* **1,** 489–495
59. Degterev, A., Hitomi, J., Germscheid, M., Ch'en, I. L., Korkina, O., Teng, X., Abbott, D., Cuny, G. D., Yuan, C., Wagner, G., Hedrick, S. M., Gerber, S. A., Lugovskoy, A., and Yuan, J. (2008) Identification of RIP1 kinase as a specific cellular target of necrostatins. *Nat. Chem. Biol.* **4,** 313–321
60. Pierdomenico, M., Negroni, A., Stronati, L., Vitali, R., Prete, E., Bertin, J., Gough, P. J., Aloi, M., and Cucchiara, S. (2014) Necroptosis is active in children with inflammatory bowel disease and contributes to heighten intestinal inflammation. *Am. J. Gastroenterol.* **109,** 279–287
61. Lek, M., Karczewski, K. J., Minikel, E. V., Samocha, K. E., Banks, E., Fennell, T., O'Donnell-Luria, A. H., Ware, J. S., Hill, A. J., Cummings, B. B., Tukiainen, T., Birnbaum, D. P., Kosmicki, J. A., Duncan, L. E., Estrada, K., *et al.* (2016) Analysis of protein-coding genetic variation in 60,706 humans. *Nature* **536,** 285–291
62. Speckmann, C., Lehmberg, K., Albert, M. H., Damgaard, R. B., Fritsch, M., Gyrd-Hansen, M., Rensing-Ehl, A., Vraetz, T., Grimbacher, B., Salzer, U., Fuchs, I., Ufheil, H., Belohradsky, B. H., Hassan, A., Cale, C. M., *et al.* (2013) X-linked inhibitor of apoptosis (XIAP) deficiency: the spectrum of presenting manifestations beyond hemophagocytic lymphohistiocytosis. *Clin. Immunol.* **149,** 133–141
63. Marsh, R. A., Madden, L., Kitchen, B. J., Mody, R., McClimon, B., Jordan, M. B., Bleesing, J. J., Zhang, K., and Filipovich, A. H. (2010) XIAP deficiency: a unique primary immunodeficiency best classified as X-linked familial hemophagocytic lymphohistiocytosis and not as X-linked lymphoproliferative disease. *Blood* **116,** 1079–1082
64. Heliö, T., Halme, L., Lappalainen, M., Fodstad, H., Paavola-Sakki, P., Turunen, U., Färkkilä, M., Krusius, T., and Kontula, K. (2003) CARD15/NOD2 gene variants are associated with familially occurring and complicated forms of Crohn's disease. *Gut* **52,** 558–562
65. Dziadzio, M., Ammann, S., Canning, C., Boyle, F., Hassan, A., Cale, C., Elawad, M., Fiil, B. K., Gyrd-Hansen, M., Salzer, U., Speckmann, C., and Grimbacher, B. (2015) Symptomatic males and female carriers in a large Caucasian kindred with XIAP deficiency. *J. Clin. Immunol.* **35,** 439–444
66. Marsh, R. A., Villanueva, J., Zhang, K., Snow, A. L., Su, H. C., Madden, L., Mody, R., Kitchen, B., Marmer, D., Jordan, M. B., Risma, K. A., Filipovich, A. H., and Bleesing, J. J. (2009) A rapid flow cytometric screening test for X-linked lymphoproliferative disease due to XIAP deficiency. *Cytometry B Clin. Cytom.* **76,** 334–344
67. Russo, H. M., Rathkey, J., Boyd-Tressler, A., Katsnelson, M. A., Abbott, D. W., and Dubyak, G. R. (2016) Active caspase-1 induces plasma membrane pores that precede pyroptotic lysis and are blocked by lanthanides. *J. Immunol.* **197,** 1353–1367
68. Gibson, D. G., Young, L., Chuang, R.-Y., Venter, J. C., Hutchison, C. A, 3rd, and Smith, H. O. (2009) Enzymatic assembly of DNA molecules up to several hundred kilobases. *Nat. Methods* **6,** 343–345